Depositional Environment and Reservoir Prospect Analysis of Barail Sandstone Exposed in the Northeastern Part of Bangladesh

Muhit Alam[1], M. Mostafizur Rahman[1*], M. Yousuf Gazi[1], Janifar Hakim Lupin[1] and Mohammad Nazim Zaman[2]

[1]Department of Geology, University of Dhaka, Dhaka 1000, Bangladesh
[2] Institute of Mining, Mineralogy and Metallurgy (IMMM), BCSIR, Joypurhat, Bangladesh

Manuscript received: 27 April 2023; accepted for publication: 12 October 2023

ABSTRACT: The study characterized the Oligocene Barail sandstone in the Surma Basin from a reservoir perspective. Data were collected by direct field observations; rock samples were collected from outcrops for detailed sedimentological, petrographic, and geochemical analysis. Collected sedimentary logs are analyzed to delineate the facies associations, sandbody architecture, and depositional environment. A total of ten facies were identified, which were further grouped into three facies associations: FA1: Tidal-influenced multistorey channel-fill deposits, FA2: Fluvial multistorey channel-fill deposits, and FA3: Overbank deposits. Facies analysis suggests that the Barail sandstone was deposited in the tidal-influenced paralic to fluvial depositional settings, and channel body dimensions increase towards the top. A petrographic study shows that these sandstones are mostly litharenite ($Q_{70}F_4L_{26}$) in type, and sediments were derived from quartzose recycled orogens. The average porosity of the sandstones is 16.9%; the pore spaces are of both primary and secondary origin and are mostly interconnected. Porosity distribution in the fluvial multistory channel-fill deposits (FA2)—the upper part of the sandstone succession, is less heterogeneous, while that in the tidal-influenced channel-fill deposits (FA1), occurs in the lower part is more heterogeneous. Both the depositional process and diagenesis influenced the porosity of Barail sandstones. Geochemical analysis suggests that the sandstones are chemically stable and moderately matured. The study demonstrates that the Barail sandstones may be a good petroleum reservoir.

Keywords: Depositional Environment; Sedimentary Facies; Petrography; Geochemistry; Reservoir Quality; Barail Sandstone; Oligocene; Surma Basin

INTRODUCTION

The Surma Basin occupies the northeastern part of the Bengal Basin (Khan et al., 1988; Islam and Jahan, 2013). The Miocene-aged Surma Group successions in this basin are the main hydrocarbon reservoirs of the country (Curray et al., 2002). The Surma Group is underlain by the Oligocene-aged Barail Group, which consists of two formations: the upper Renji Formation (arenaceous) and the lower Jenum Formation (argillaceous) (Evans, 1932). The Jenum Formation is reported as the petroleum source rock in the basin (Riemann and Hiller, 1993; Evans, 1932). If the Barail sandstones (Renji Formation) satisfy all the requirements of the reservoir and the lower part successions of the Surma Group (Bhuban Formation) act as a seal, there is a significant potential to occur natural gas within this sandstone unit. In Assam geological province, the arenaceous succession of the Barail Group (Renji Formation) contains extensive oil reserves and the reservoir quality of these sandstones is high (Bezbaruah, 2014; Borgohain et al., 2021). Hydrocarbons have been produced from the arenaceous units of the Barail Group in the Upper Assam Basin for more than a century (Borgohain et al., 2010).

Previous studies suggest that the Oligocene Barail sandstones are deposited in the fluvial to deltaic depositional environments, which represents the progradation of the delta (Alam, 1989; Johnson and Alam, 1991). The prominent lithofacies of the sandstone are fine to coarse-grained parallel, ripple-cross, and trough-cross-stratified sandstones (Khanam et al., 2021). The textural properties of the deposits, the presence of thin coal fragments, and clay galls point to a possible terrestrial origin for this deposit (Srivastava and Pandey, 2011; Khanam et al., 2021). Numerous

[*] Corresponding Author: M. Mostafizur Rahman
Email: mostafiz2021@du.ac.bd
DOI: https://doi.org/10.3329/dujees.v12i1.70557

studies have been carried out on the petrographic composition of the sandstone unit both in the Assam Basin and Surma Basin (Dickinson and Suczek, 1979; Dickinson, 1985; Uddin and Lundberg, 1998; Hossain et al., 2010). Johnson and Alam (1991) and Uddin and Lundberg (1998) suggested that Barail Group sandstones are sublitharenite to quartzarenite derived from a recycled orogen. Quartz grains are dominantly monocrystalline, subangular to subrounded in shape; the polycrystalline quartz grains contain chert (Uddin and Lundberg, 1998). Lithic fragments are dominant in the Barail Group; the grains are primarily sedimentary (avg. Ls/L=0.53) and metamorphic (avg. Lm/L=0.46) (Hossain et al., 2010). The amount of feldspar is lower in the Barail sandstone, which indicates mixed sedimentary and metamorphic sources (Hossain et al., 2010). K-feldspar is more prominent than plagioclase feldspar, mostly orthoclase and microcline (Hossain et al., 2010). The sources of sediments are mostly sedimentary and metamorphic rocks exposed to erosion by the orogenic uplift of the Himalayas (Borgohain et al., 2019; Srivastava and Kichu, 2022). A 4-meter thick laterite bed in the upper surface of the Barail Group indicates a major transgressive unconformity surface (Khanam et al., 2021). Islam et al. (2021) suggested that the density of sandstones ranges from 1.94 g/cm3 to 2.37 g/cm3, and average porosity and permeability are 16.48% and 132.48 mD, respectively. Little work has been done to study the detailed sedimentology, sandbody stacking pattern, and diagenesis and their link to the reservoir properties of the sandstones. The present work aims to study the sedimentology, petrography, and geochemistry of the Barail sandstones to understand the depositional environment and reservoir properties and to evaluate its reservoir prospects.

GEOLOGICAL SETTINGS

The Surma Basin, also known as Sylhet Trough, is located in the northeastern part of the Bengal Basin (Fig. 1). The trough covers an area of approximately 2.5 million acres. It subsides primarily between the Oligocene and Pliocene epochs (Hiller, 1984). The Surma Basin is a tectonically complex region (Lietz and Kabir, 1982). It is fringed to the north by the Shillong Plateau, where the east-west trending Dauki Fault is deemed the borderline (Johnson and Alam, 1991). On the east and southeast, the trough is bounded by the frontal zone of the Chittagong-Tripura Fold Belt (CTFB) and on the west by the stable platform. It is open to the south and southwest of the major section of the Bengal Basin (Hiller, 1984).

The Sylhet Trough had a complex evolutionary history demonstrating a change from a passive and rifted continental setting to a flexural foreland basin (Alam et al., 2003). The formation of the trough is linked to two major tectonic events: i) pop-up of the Shillong Plateau in the northern part of the trough and ii) oblique subduction of the Indian plate below the Burmese plate (Johnson and Alam, 1991; Islam et al., 2021). The late Mesozoic and Cenozoic stratal thickness in the Sylhet Trough has been estimated to be between 13 and 17 km, with much of this layer being Neogene in age (Evans, 1964; Hiller, 1984; Fig. 1). During the late Mesozoic to the Eocene, the Sylhet Trough area was lying on a slope setting on a passive continental margin where the Jaintia Group (Tura Sandstone, Sylhet Limestone and Kopili Shale formations) successions were deposited. In Oligocene time, the subsidence might have increased slightly when the trough was positioned in the distal portion of a foreland basin in front of the Indo-Burman Mountains (Evans, 1964; Hiller, 1984). The Oligocene fluvio-deltaic successions, called Barail Group, were deposited from sediments from early-stage uplifts in the eastern Himalayas (Evans, 1964; Hiller, 1984; Alam, 1989). Subsidence occurred extensively during the Miocene as a result of the western advancement of the Indo-Burman Range (IBR) when the Surma Group sediments were deposited in a vast, mud-rich delta system that may have drained a considerable area of the eastern Himalayas (Hiller 1984; Johnson and Nur Alam 1991; Parvin et al. 2019) electrofacies and depositional sequences were interpreted from wire line logs. Then, the field wide configurations of these sequences have been identified in seismic using reflection terminations (offlap, onlap, top lap and down lap relationship. Subsidence rates in the trough increased substantially from the Miocene to the Plio-Pleistocene, when the fluvial successions of Tipam Sandstone, Girujan Clay, and Dupi Tila formations, and glacial outwash deposits of Dihing Formation were deposited (Alam 1989; Johnson and Nur Alam 1991).

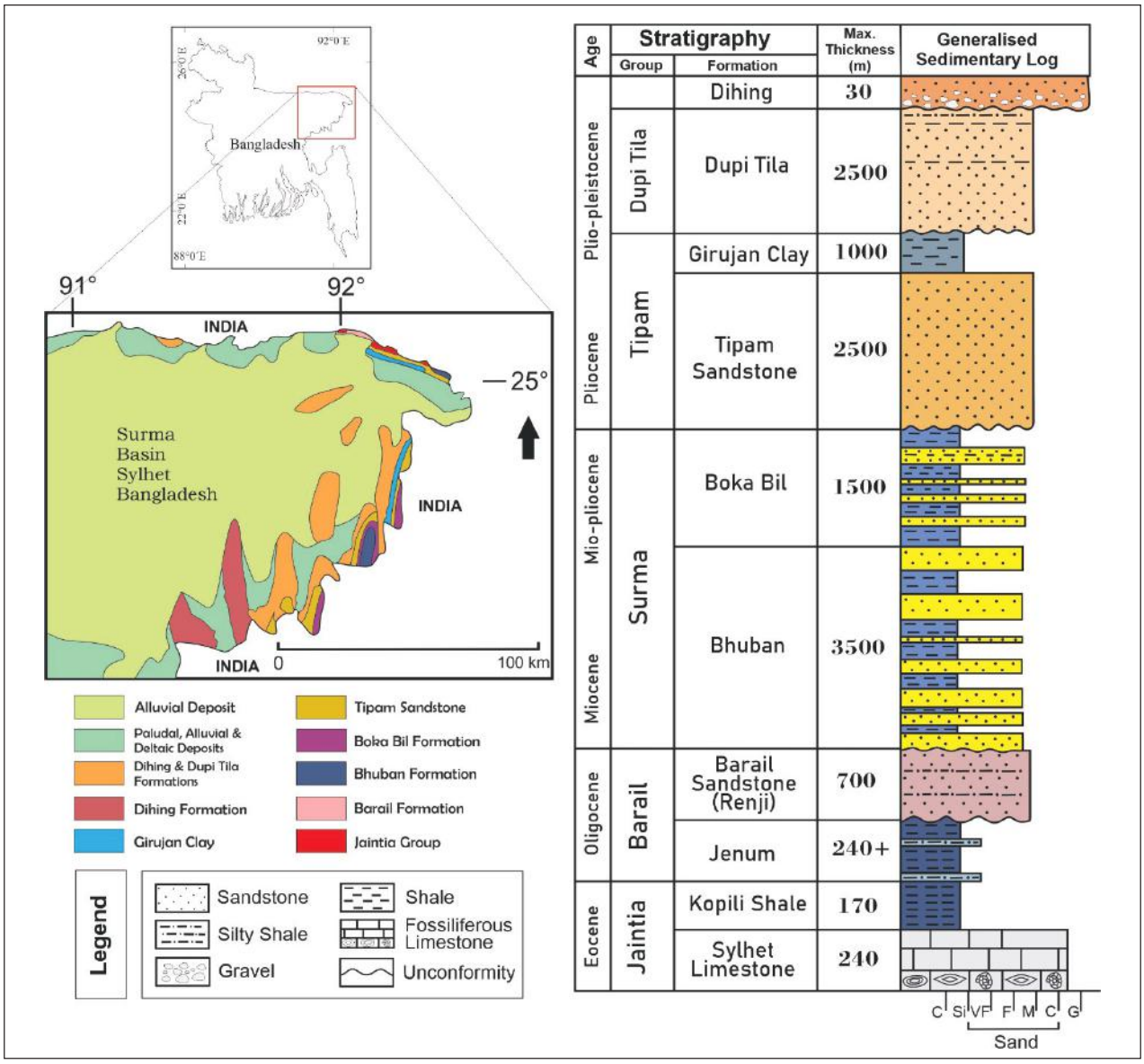

Figure 1: Geological Map Shows Stratigraphic Units in the Surma Basin (Left) and Generalized Stratigraphic Succession (right; modified from Alam et al., 1990 and Imam, 2013)

DATA AND METHODS

The study used outcrop data to analyze the sedimentological characteristics and petrographic and geochemical properties of the Barail sandstone. The detailed datasets and methods are described below.

Outcrop Study

A total of six outcrops sections: Jaflong, Tamabil, Noljhuri, Rangapani, Gourishankar, and Lalakhal were selected for sedimentary logging and sample collection, which are located in the Jaflong-Jaintapur area, Sylhet (Fig. 2). Field investigations primarily focused on recognizing and mapping various lithofacies units, identifying and measuring stratigraphical and lithological attributes (i.e., the colour, granularity, rock-type, thickness of beds, weathering, the attitude of beds, etc.), identifying lithological contacts, and recognizing structural features. It involved traversing along the road- and river-cut sections. A total of 11 samples were collected from the 11 stations of six outcrop sections (Fig. 2) for laboratory analysis. Fresh sandstone samples were collected from the studied outcrop sections by digging down to unaltered rock layers, adopting the methodology of Trendell et al. (2012).

Petrographic Study

The rock samples were carefully labelled and packed for safe transportation and subsequent laboratory analysis. Thin section preparation of the sandstone samples was carried out in the Sedimentology and Petrography Laboratory at the Department of Geology, University of Dhaka. Out of eleven representative samples, ten thin sections were prepared for the petrographic study.

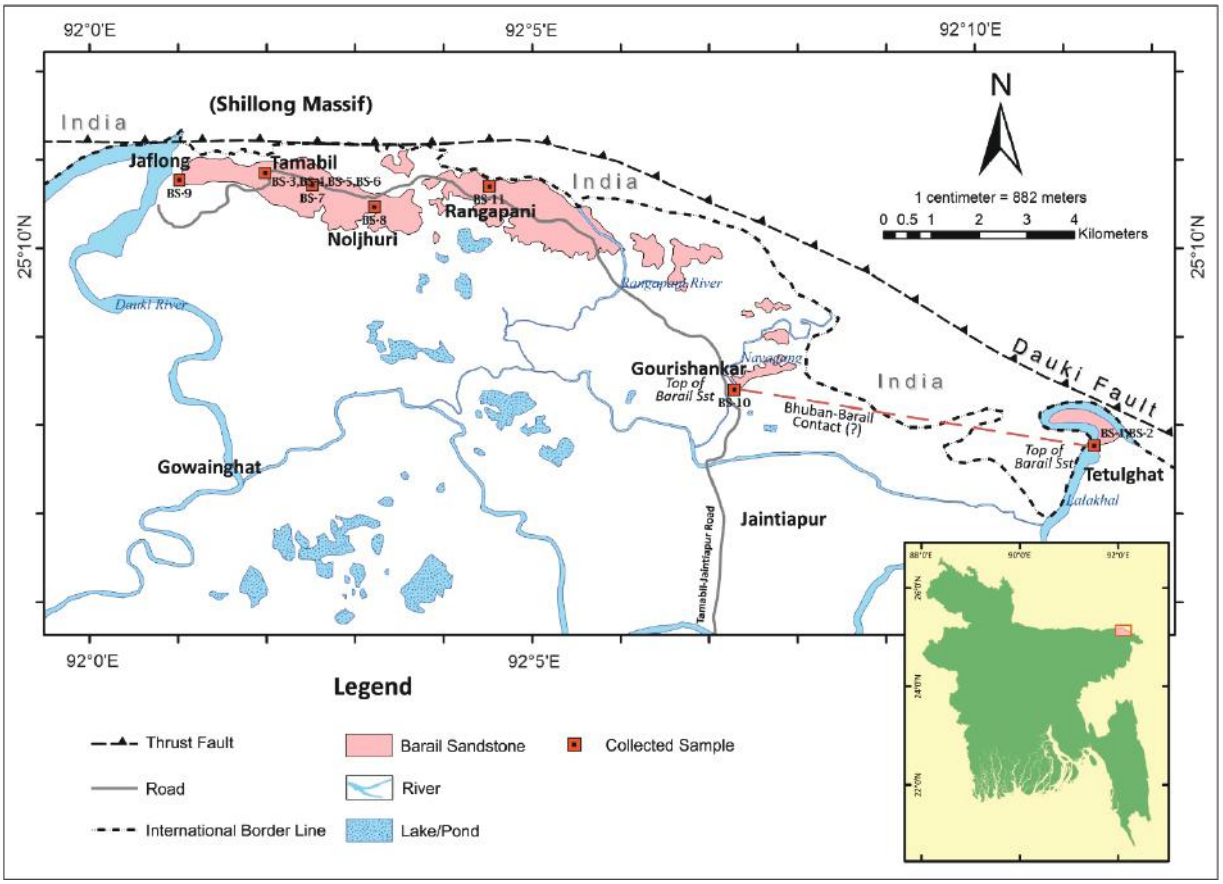

Figure 2: Map Shows the Location of Exposed Barail Sanstone and the Studied Stations

The samples were initially sliced into little chips by a rock-cutting machine to prepare standard thin sections. The chips were dried to remove their liquid content and then impregnated with blue dye. The thin section slides were prepared following the standard procedure. After preparing thin sections, samples were investigated under a petrographic microscope to observe grain morphology, texture, grain types, and porosity with other petrographic characteristics. The rock texture, composition, and rock classification were determined by petrographic analysis, and quantitative measurement of porosity and qualitative estimation of permeability were recorded.

Geochemical Study

In the study, the Rigaku ZSX Primus XRF machine was used for the X-ray fluorescence (XRF) Spectrometric analysis of the powder samples to study the geochemistry of samples and describe the tectonic setting, provenance, weathering history, and maturity of sandstones. Based on the collected datasets, various geochemical classification diagrams were prepared and analyzed. Herron's (1988) classification diagram, Roser and Korsch's (1986) discrimination diagram, Suttner and Dutta's (1986) bivariant plot, binary variation diagrams, etc., were used to analyze the dataset in this study. The degree and duration of weathering of the deposits are analyzed by examining the interactions between alkali and alkaline earth elements. Various

diagrams are analyzed to define source area weathering, the transformation of plagioclase into clay minerals, and the composition of the source rock. Those are the Chemical Index of Alteration (CIA), the Chemical index of weathering (CIW), the Plagioclase Index of Alteration (PIA), and the several ratios of SiO_2/ Al_2O_3, Al_2O_3/K_2O, K_2O/Na_2O.

RESULTS

Facies Analysis

Lithofacies characteristics of the succession are studied in the sedimentary logs prepared in the outcrop sections. The studied lithofacies and facies associations are described in this section.

Lithofacies

A total of ten lithofacies are identified in the studied sections which are summarized in Table 1 and Figure 3. The description of each lithofacies is given below.

Intraformational Conglomerate (C_{IF})

Intraformational conglomerate (C_{IF}) facies is reddish brown coloured to mottled, structureless, and wedge-shaped in nature. The clasts are granule to pebble-sized, poorly sorted, subrounded to rounded in shape and composed of mudstone (Fig. 3A), and the matrix materials are sandy. They occur above the scoured surface and are overlain by trough cross-stratified sandstone ($\mathbf{S_{TXS}}$) facies. The facies was studied at the Lalakhal section near the Bangladesesh-India border area.

The occurrence of the facies above the scouring surface and beneath the $\mathbf{S_{TXS}}$ facies suggests that they are deposited at the base of the channel as lag deposits. The muddy materials of the clasts suggest their intraformational origin. They represent rapid deposition from high energy conditions (Ghosh et al., 2015).

Lateritic Conglomerate (C_L)

Lateritic conglomerates (C_L) facies is yellowish to reddish-brown coloured, chaotic, massive, and vesicular in structure (Fig. 3B). It consists of clasts of mostly pebble sized along with a few granule and cobble sized and matrix of ferruginous medium to coarse-grained sands which are coated by iron crust. The clasts are mostly composed of quartz grains along with a few muddy materials. Where laterization is moderate to low, it shows the trough cross-bedded sedimentary structure. Up to 4m thick C_L facies are studied at the uppermost part of the successions at the Gourishankar area in the Nayagang river-cut section and the Noljhuri section beside the Jaflong-Tamabil road.

The Surma Group deposits overlie the studied succession. Oligocene marine regression exposed the upper Barail successions, which then experienced weathering and laterization in a warm and humid climate where the water table fluctuated. The grain size and sedimentary structure (studied in the low laterized areas) suggest that the laterization process occurred in the tough-cross stratified (S_{TCS}) channel-fill facies.

Massive Sandstone (S_M)

Massive sandstone ($\mathbf{S_M}$) facies is grey to light pink colored, fine to medium-grained, moderately sorted, and structureless sandstone (Fig. 3C). The thickness of the facies ranges from 30 cm to 1 m. These facies are studied in the Tamabil and Lalakhal sections.

Rapid deposition of sediments from suspension through gravity settles in the absence of traction due to the sudden drop of flow energy forming the facies (Martin and Turner, 1998; Rahman et al., 2022). The facies develops when a considerable amount of sediment is deposited over a very short time. In the fluvial channel, the facies occurs during high energy conditions when a huge amount of sediment load is carried by water and these overloaded sediments are deposited rapidly. Therefore, sediments do not get enough time to develop any internal structure.

Planar Cross-stratified Sandstone (S_{PXS})

Planar cross-stratified sandstone (S_{PXS}) facies is composed of yellowish-brown colored, fine to medium-grained planar cross-stratified sandstone (Fig. 3D). Coset thicknesses of planar cross-bedded sandstone units range from 1 m to around 2 m. The facies is studied in the Nayagang and Jaflong sections. Planar cross-bed sets are common in granular sediments, particularly

sandstone, and are deposited from the 2D straight/long crested dune migration within the channel.

Trough-cross Stratified Sandstone (S_{TXS})

Trough-cross stratified sandstone (S_{TXS}) facies is composed of yellowish-brown colored, fine to medium-grained, trough cross-bedded sandstone (Fig. 3E). Occasionally, mud balls are observed at the tangential part of the trough sets. The thickness of individual trough-cross stratified units ranges from 30 cm to 1 m, and coset thickness was recorded up to 13 m. The facies is studied in the Nayagang and Lalakhal sections. Migration of three-dimensional (3D) curve crested dunes generates this type of facies.

Parallel Laminated Sandstone (S_{PL})

Parallel laminated sandstone (S_L) facies is composed of yellowish to gray coloured, fine to medium-grained sand with parallel lamination (Fig. 3F). S_L facies is found at the top of the channel sand in the Tamabil and Nayagang sections. The thicknesses of this unit range from 20 cm to 50 cm. Generally, traction transport generates this type of facies. This facies indicates a steady current in the lower part of the lower flow regime.

Ripple Cross-stratified Sandstone (S_{RXS})

Ripple cross-stratified (S_{RXS}) sandstone facies contain yellowish to reddish-brown coloured, fine to medium-grained sand, with clay galls (Fig. 3G). The trough of the ripples contains isolated mud drapes. These facies are found in the Tamabil and Jaflong sections. These facies are developed in settings where abundant sediment supply and traction are present, causing the migration of ripples. The mud drapes suggest the deposits may form in a tidal-influenced depositional condition.

Lenticular Stratified Heterolithic (H_{LS})

Lenticular stratified heterolithic (H_{LS}) facies comprises grey-coloured mud with lenses of yellowish-coloured silt to very fine sand where the proportion of mud is relatively higher (Fig. 3H). This facies is studied below the channel bodies in the Tamabil section. The thickness of the facies ranges from 0.5 m to 1 m. The facies is deposited by decreasing flow velocity from suspension in floodplains where mud dominates, and sand or silt is deposited above the mud units as ripples. This facies is developed during the period of quiescence with decreasing flow velocity.

Poorly Laminated Shale (F_{PL})

The facies consist of gray-coloured, poorly laminated, fissile shale with tiny silt streaks in the lamination plane (Fig. 3I). The thickness of the facies decreases upward, ranging from 15 cm to 1 m. The facies is studied in the Jaflong and Lalakhal sections. This facies is deposited from suspension on the floodplain. When the energy of sediment-laden flow decreases, the sediments start to settle down, and finer particles settle down at the later stage from suspension on the floodplain.

Mudstone with Coal Lenses (M_C)

The facies consists of dark grey to mottled, clay to silt-sized grains with coal lenses. Poor laminations are occasionally observed (Fig. 4.1J). Coal lenses are very thin, discontinuous, and slightly concave upward in shape. The thickness of the facies ranges from 1 to 2.5 m. This facies is studied in the Tamabil section. The dark grey to the mottled colour of the facies, along with the presence of coal lenses, suggests that these facies were deposited in the low-lying floodplain or delta top swampy area where vegetation grew in-situ or drifted from elsewhere with floodwater flow that was submerged or deposited by the floodwater and buried under fine grain sediments, those eventually turned into coals due to burial and compaction and form coal lenses within mud units.

Table 1: Lithofacies Scheme of the Studied Barail Sandstone Successions

Code	Facies	Lithology	Basal Contact	Process of Deposition
C_{IF}	Intraformational conglomerate	Reddish brown coloured to mottled, structureless, wedge-shaped and granule to pebble-sized, poorly sorted, subrounded to rounded muddy clasts with sandy matrix	Irregular, scoured surface	Deposited at the base of the channel as lag deposits.
C_{L}	Lateritic conglomerate	Yellowish to reddish brown coloured laterites with subrounded to well-rounded quartz clasts (pebbles, many granules, and intermixed cobbles)	Irregular surface	Lateralization of sandstones during marine regression
S_{M}	Massive sandstone	Yellowish gray to light pink coloured, fine to medium-grained, moderately sorted, and structureless sandstone with clay galls	Flat surface	Deposited through gravity, settle in fluvial channels
S_{PXS}	Planar cross-stratified sandstone	Yellowish-brown coloured, fine to medium-grained sand with medium-scaled planar cross-stratified bedding	Flat, sharp surface	Deposited from 2D straight/long crested dune migration
S_{TXS}	Trough cross-stratified sandstone	Yellowish brown to gray coloured, fine to medium grained, trough cross-stratified sandstone with lignite fragments and mud pebbles	Flat, sharp surface	Deposited from the migration of three-dimensional (3D) curve crested dunes
S_{L}	Laminated sandstone	Yellowish to gray coloured, fine to medium grained, parallel lamination sandstone	Flat surface	Deposited from steady current in the lower part of the lower flow regime in the fluvial channel
S_{RXS}	Ripple cross-stratified sandstone	Yellowish to reddish-brown coloured, fine to medium-grained sandstone with mud drapes and clay galls	Irregular surface	Deposited by current flow
H_{LS}	Lenticular stratified heterolithic	Grey coloured mud with lenses of yellowish coloured silt to very fine sand	Flat surface	Evidence of floodplain deposit
F_{PL}	Poorly laminated shale	Gray coloured, poorly laminated, fissile shale with highly fissile shale with tiny silt streaks in the lamination plane	Flat surface	Deposited from suspension in floodplain
M_{C}	Mudstone with coal lenses	Dark grey to mottled, clay to silt-sized grains with coal lenses	Flat surface	Deposited in low-lying floodplain or delta top swampy area

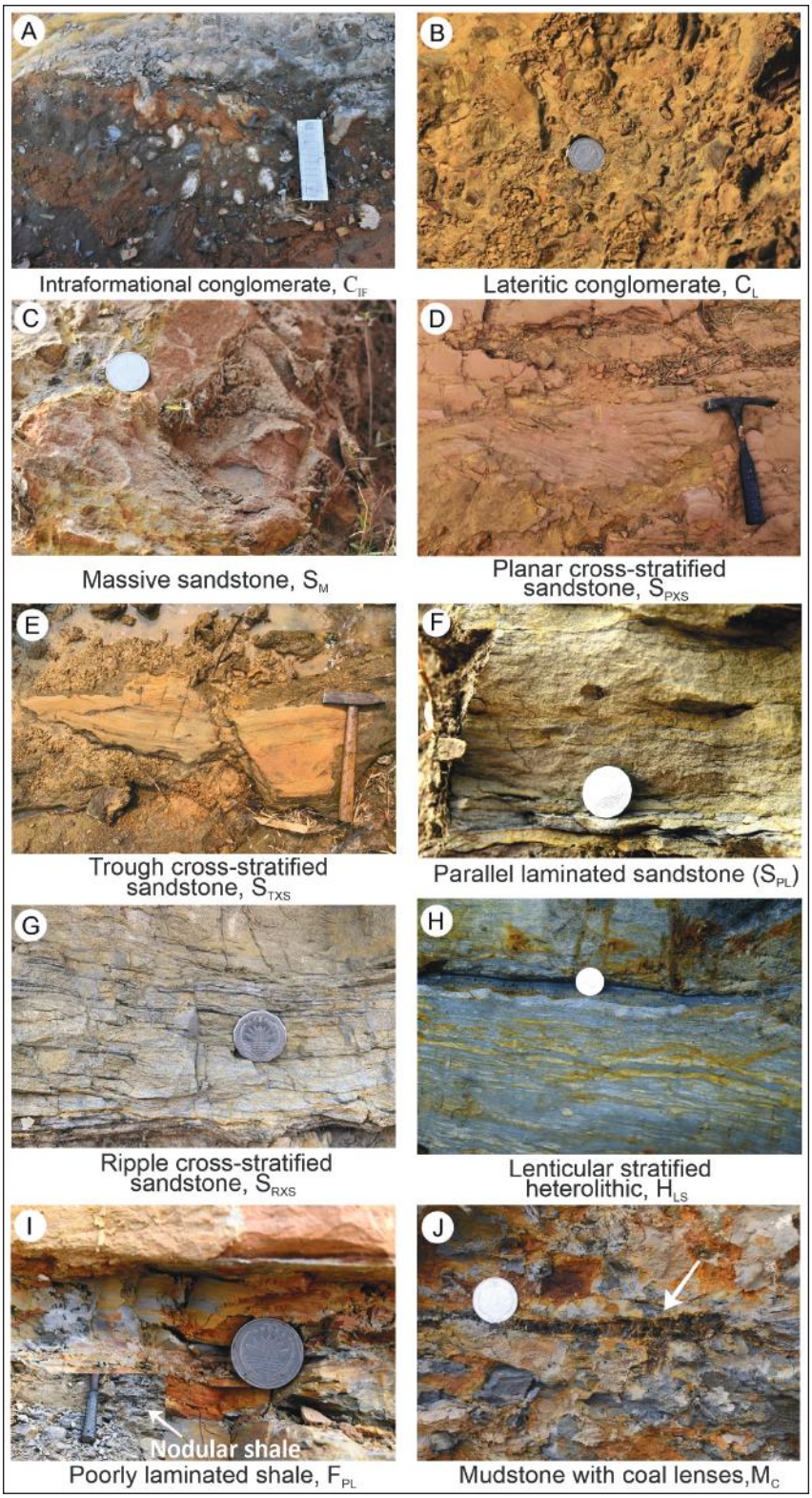

Figure 3: Photographic Examples of Studied Facies: (A) Intraformational Conglomerate (C_{IF}) Facies, (B) Lateritic Conglomerate (C_L) Facies, (C) Massive Sandstone (S_M) Facies, (D) Planar Cross-stratified Sandstone (S_{PXS}) Facies, (E) Trough-cross-stratified Sandstone (S_{TXS}) Facies, (F) Laminated Sandstone (S_L) Facies, (G) Ripple Cross-stratified Sandstone (S_{RXS}) Facies, (H) Lenticular Stratified Heterolithic (H_{LS}) Facies, (I) Poorly Laminated Shale (F_{PL}) Facies and (J) Mudstone with Coal Lenses (M_C) Facies

Facies Association

The studied facies are grouped into three facies associations: FA1: Tidal-influenced multistorey channel deposits, FA2: Fluvial multistorey channel deposits, and FA3: Overbank deposits (Fig. 4). The facies associations are described in the following section.

FA1: Tidal-influenced Multistorey Channel Deposits

FA1 is consisted of yellowish grey to pinkish yellow coloured fine to medium-grained sandstone facies: S_M, S_{TXS}, S_{PXS}, S_{RXS}, and S_L. The sandstones are trough and planar cross-stratified, ripple cross-stratified, and plane-parallel laminated in structure with mud drapes and clay galls (Fig. 3 and 4). The ripple cross-stratified sandstone shows a bidirectional paleocurrent pattern. Sandstone beds occasionally show a structureless pattern with poorly developed normal grading. It shows a fining upward sequence from massive sandstone facies and/or cross-stratified sandstone facies–laminated sandstone facies. Individual channel-fill deposits are 0.5–2.5 m thick and 5–25 m wide. The deposits show a multistorey stacking pattern, and the individual channels are concave-upward erosionally based. The channel bodies are not fully exposed. In this study, up to 100 m wide channel body is recorded. This facies association is studied in the Jaflong and Tamabil road-cut sections.

The sedimentological characteristics, along with mud drapes and bidirectional sedimentary structure within sandstone facies, suggest that FA1 was deposited within channels near the palaeoshoreline in the influence of a degree of tidal process.

FA2: Fluvial Multistorey Channel Deposits

FA2 consists of intraformational conglomerate (C_{IF}), lateritic conglomerate (C_L), and trough cross-bedded (S_{TXS}), ripple cross-stratified (S_{RXS}), and parallel laminated sandstone (S_L) facies. The lateritic conglomerate facies occurs at the upper part of the channel deposits. The facies association consists of fine to medium-grained sandstone with abundant mud balls and occasional quartz pebbles. The storey surfaces are concave-upward erosional scour which are overlain by intraformational conglomerate facies. The preserved storey thickness ranges from 0.5–5 m. The actual channel thickness was not possible to determine as the younger channels cut the older ones and were stacked. The whole channel bodies are not exposed in the studied sections. A multistorey channel section up to 50 m thick was studied in the Gourishankar area along the Nayagang river-cut section. Along with the Nayagang section, this facies association was studied in the Lalakhal and Rangapani sections (Fig. 4).

The presence of traction current-dominated sedimentary structures, several storey surfaces and thick sandy nature devoid of mud drapes suggest that channel amalgamation forms the multistory stacking pattern of the channel body in the fluvial depositional environment.

FA3: Overbank Deposits

The overbank facies association (FA3) is constituted of grey, dark grey, and mottled, lenticular stratified heterolithic (H_{LS}), poorly laminated shale (F_{PL}), and mudstone with coal lenses (M_C) facies. The mudstone occasionally contains sporadic silt to very fine-grained sandstone lamina. In some places, they show coal lenses. The facies association is found in the Tamabil and Jaflong sections. The laterally continuous mudstone and heterolithic deposits suggest an overbank origin. When the distributary channels got flooded, overbank facies were developed.

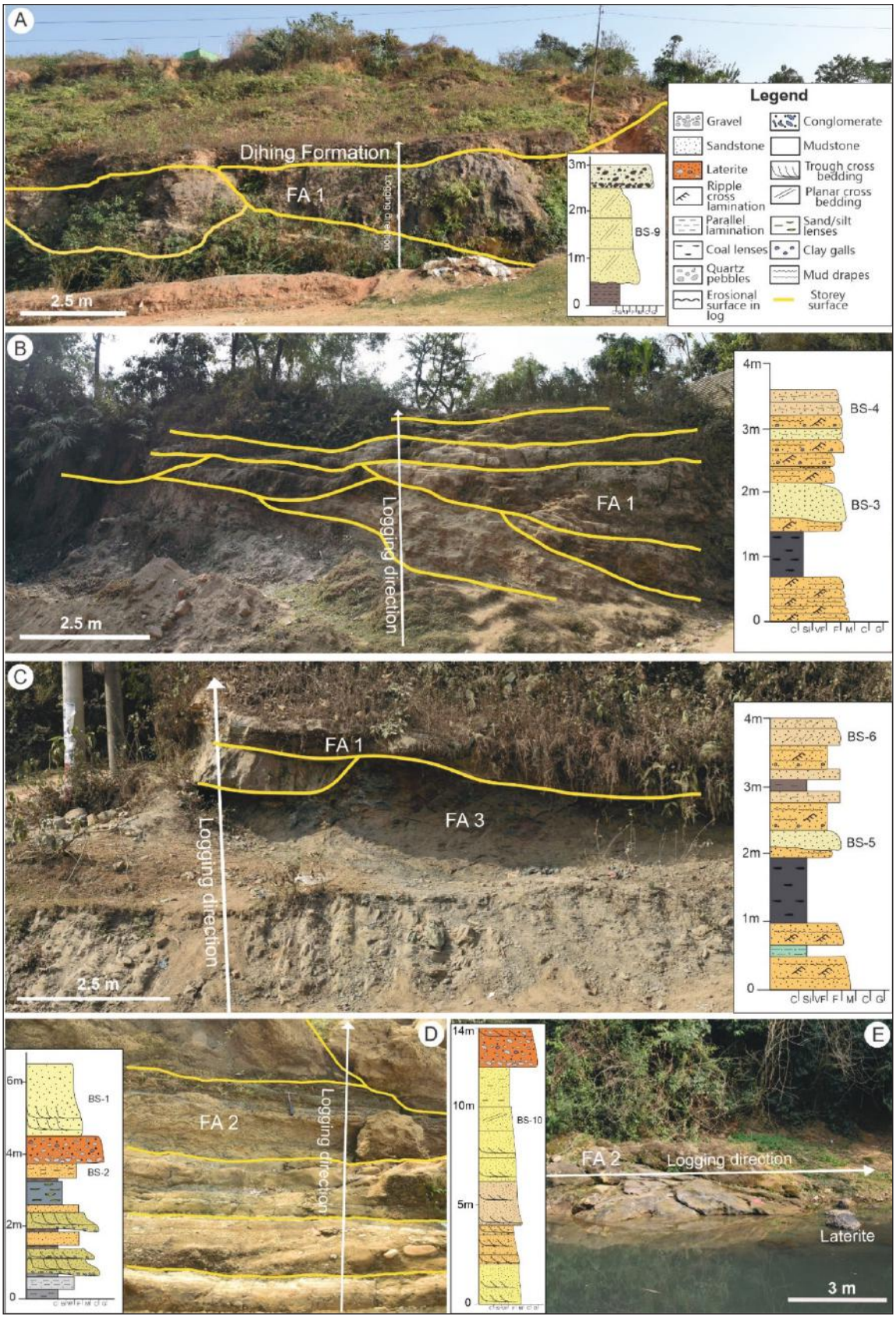

Figure 4: Examples of Facies Associations in the (A) Jaflong Section, (B) Tamabil Section (Western Part), (C) Tamabil Section (Eastern Part), (D) Tetulghat Section, and (E) Nayagang Section

Petrographic Analysis

The thin section petrography of the Barail sandstones shows that the grains are mostly sub-rounded with a few sub-angular grains and moderately sorted (Fig. 5A & B). The samples mainly consist of quartz, feldspar, mica, and lithic grains (Table 2; Fig. 5). The average proportions of quartz, feldspar, mica, and lithic grains are 46.7%, 2.8%, 3.4%, and 20.8% respectively. Most of the quartz grains are monocrystalline with a few polycrystalline grains (Fig. 5B). The majority of feldspars are alkali feldspar (mainly orthoclase and microcline) with a minor proportion of plagioclase feldspar (Fig. 5C). Most of the micas are biotite and a few of them are diagenetic mica and the bending of mica flakes is also observed in a few samples (Fig. 5D). Lithic grains in the studied samples are mostly mudstone lithic grains and few mica schists and perthite lithic grains (Fig. 5F, G, & H). The grain-to-grain contacts are mostly point, long, sutured, and concavo-convex (Fig. 5E & F). The cementing materials in the samples are primarily ferruginous with a minor amount of calcareous cement (Fig. 5G & I).

From the QFL (Q: quartz, F: feldspar, and L: lithic grains) diagram, all Barail sandstone samples are classified as Litharenite except for BS-1, which is Feldspartic Litharenite (Fig. 6A). Data plotted on the tectonic discrimination diagram of Dickinson and Suczeck (1979) shows that all the samples are recycled orogeny origin (Fig. 6B)

The porosity of the studied samples ranges from 8–22% (avg. 16.9%) and pore spaces are mostly interconnected (Table 2; Fig. 5E). Samples from the upper part of the Barail sandstone (FA2) show porosity ranges from 16–22% with a standard deviation (SD) of 3.22 whereas samples from the lower Barail (FA1) show porosity ranges from 8–22% with a standard deviation (SD) of 5.50.

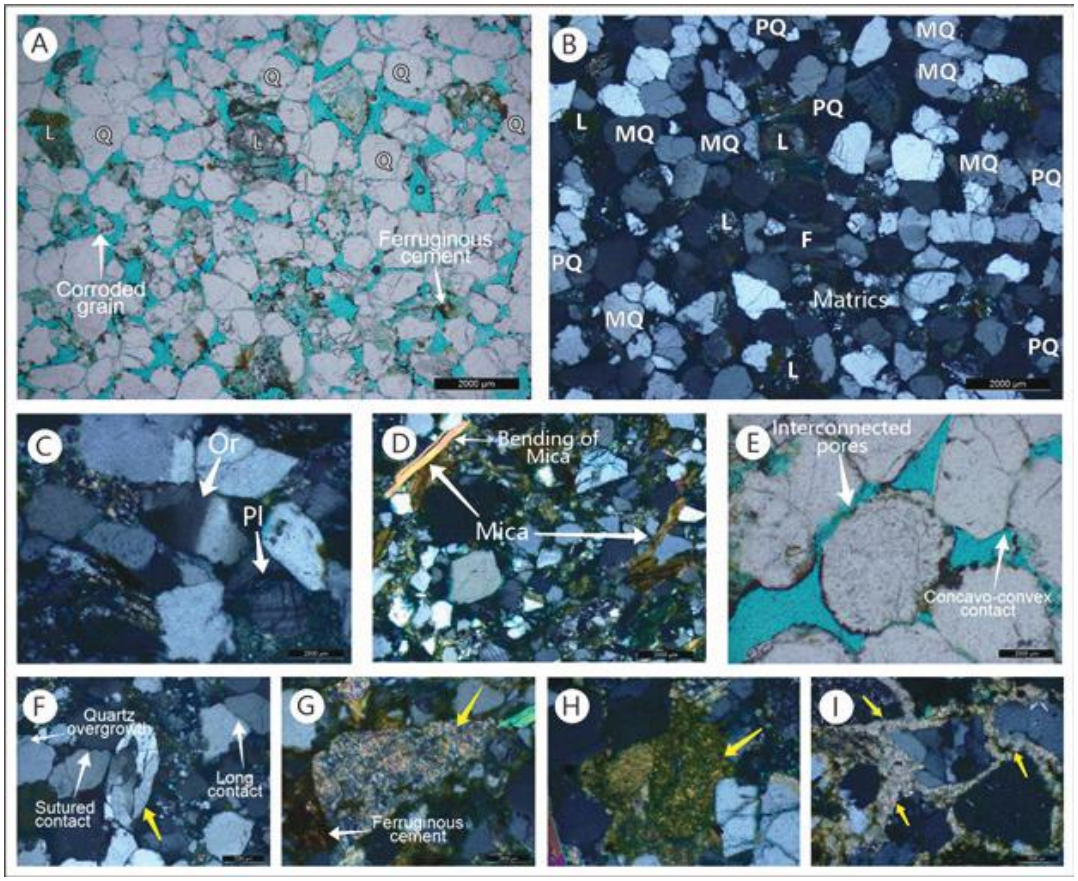

Figure 5: (A) Photomicrographs of Thin Section Slide No. BS-4 (Channel Sand of Tamabil Road-cut Section) Shows Composition of Samples Under Plane Polarized Light (PPL; 10x10X), (B) Composition of the Same Sample Under Cross Polarized Light (XPL; 10x10X), (C) Feldspar Grains Inder XPL (10x20X), (D) Mica Bending Under XPL (10x20X), (E) Interconnected Pores between the Framework Grains Under PPL (F) Perthite Lithic Grain (yellow arrow) Under XPL (10x20X), (G) Mudstone Lithic Grain (yellow arrow) Under XPL (10x20X), (H) Mica Schist (yellow arrow) Under XPL (10x20X), (I) Carbonaceous Cement (yellow arrow) between Framework Grains

Table 2: Percentage of Framework Grains, Lithicgrains, Matrix, Cementing Elements, and Porosity of the Barail Sandstones

Sample ID	FA	Quartz (%)	Feldspar (%)	Lithic grains (%)	Mica (%)	Heavy minerals (%)	Matrix (%)	Cementing Elements (%)	Porosity (%)
BS-1	**FA2**	44	7	16	6	1	10	0	16
BS-2	**FA2**	48	5	22	2	1	3	2	17
BS-3	**FA1**	46	3	22	3	2	4	0	20
BS-4	**FA1**	48	4	18	0	1	6	1	22
BS-5	**FA1**	48	1	22	2	1	7	1	18
BS-6	**FA1**	42	2	22	6	2	3	2	21
BS-7	**FA1**	48	2	20	3	2	6	4	15
BS-8	**FA1**	52	2	24	2	3	5	2	10
BS-9	**FA1**	49	1	25	5	3	4	5	8
BS-10	**FA2**	42	1	17	5	3	5	5	22

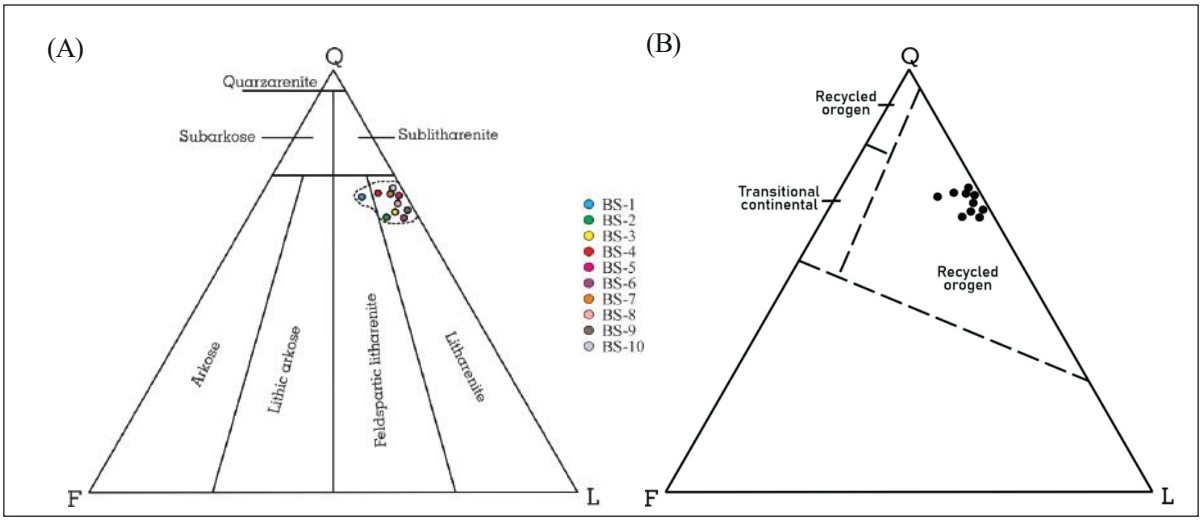

Figure 6: (A) QFL Classification of Barail Sandstones after McBride (1963) and Dott (1964) , (B) Tectonic Discrimination Plot (QFL ternary plot) of Barail Sandstone Samples after Dickinson and Suczeck (1979)

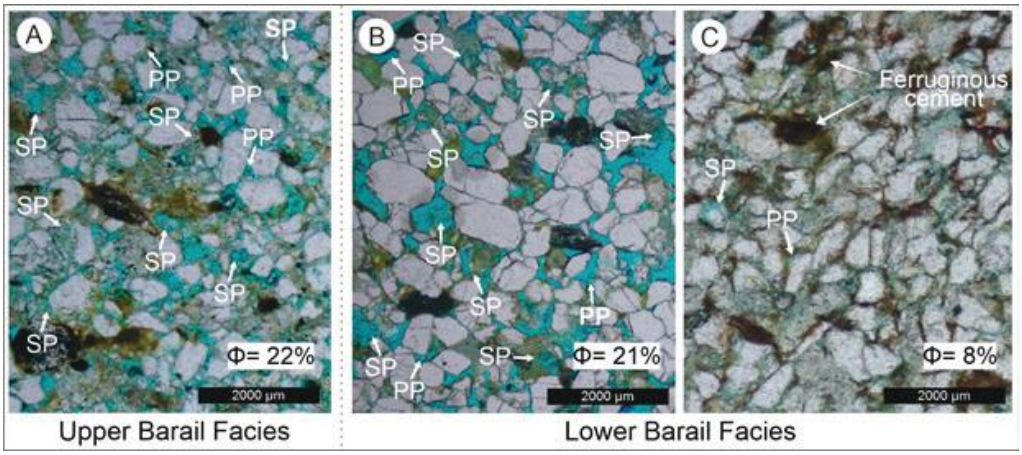

Figure 7: Photomicrographs of Thin Section Shows Porosity Distribution in (A) Upper Barail Facies (FA2) and (B & C) Lower Barail Facies (FA1) Under Planepolarized Light (4x). PP: Primary Porosity; SP: Secondary Porosity

Geochemistry

Major elemental geochemistry provides insight into the origin type and weathering conditions, both of which are influenced by the basin's tectonic context. The major oxides (in wt. %) of the Barail sandstone derived from the XRF analysis are given in Table 3.

Table 3: Major Oxides Compositions (Wt. %) and Ratios of Analyzed Barail Sandstones in the Surma Basin

Oxd. Comp.	BS-1	BS-2	BS-3	BS-4	BS-5	BS-6	BS-7	BS-8	BS-9	BS-10	BS-11
SiO_2	69.789	70.218	85.147	81.647	83.194	85.284	81.033	77.267	76.725	72.576	69.033
TiO_2	0.906	0.418	0.817	0.920	0.818	0.783	0.788	0.771	1.363	0.917	1.556
Al_2O_3	13.761	10.921	7.834	10.573	8.535	7.765	10.696	9.801	15.644	16.019	17.856
Fe_2O_3	7.937	7.132	2.989	3.003	3.663	3.249	4.567	8.789	2.815	5.586	6.576
MnO	0.079	0.201	0.025	0.029	0.021	0.026	0.019	0.038	0.029	0.086	0.033
MgO	1.057	1.587	0.536	0.510	0.651	0.330	0.293	0.243	0.297	0.844	0.591
CaO	0.788	3.996	0.046	0.119	0.071	0.089	0.086	0.122	0.065	0.186	0.105
Na_2O	1.266	1.231	0.240	0.183	0.315	0.193	0.169	0.245	0.203	0.144	0.104
K_2O	3.322	3.086	1.817	2.173	1.946	1.597	1.742	1.445	2.345	2.749	3.309
P_2O_5	0.100	0.111	0.029	0.033	0.038	0.030	0.039	0.164	0.059	0.129	0.069
NiO	0.022	0.019	0.010	0.012	0.000	0.008	0.011	0.014	0.007	0.016	0.014
ZnO	0.016	0.011	0.006	0.000	0.006	0.000	0.000	0.000	0.006	0.011	0.009
CuO	0.000	0.000	0.007	0.000	0.000	0.000	0.007	0.008	0.007	0.000	0.008
Rb_2O	0.018	0.016	0.007	0.009	0.008	0.009	0.008	0.006	0.009	0.014	0.022
SrO	0.025	0.027	0.007	0.009	0.008	0.007	0.008	0.007	0.011	0.008	0.007
ZrO_2	0.045	0.022	0.051	0.065	0.056	0.052	0.043	0.031	0.100	0.086	0.145
Nb_2O_5	0.000	0.000	0.004	0.003	0.000	0.000	0.004	0.005	0.000	0.000	0.000
Y_2O_3	0.000	0.000	0.000	0.000	0.000	0.000	0.000	0.000	0.016	0.020	0.034
BaO	0.080	0.000	0.000	0.000	0.000	0.000	0.000	0.000	0.000	0.104	0.000
NiO	0.022	0.019	0.010	0.012	0.000	0.008	0.011	0.014	0.007	0.016	0.014
SO_3	0.052	0.104	0.087	0.031	0.302	0.046	0.035	0.060	0.025	0.018	0.098
Cl	0.210	0.170	0.082	0.148	0.060	0.016	0.000	0.188	0.032	0.009	0.062
CIA	71.907	56.779	78.837	81.027	78.541	80.514	84.266	84.397	85.686	83.879	83.540
CIW	87.011	67.630	96.473	97.220	95.677	96.490	97.671	96.388	98.315	97.983	98.841
PIA	83.558	59.982	95.457	96.526	94.471	95.621	97.230	95.790	98.023	97.576	98.582
SiO_2/Al_2O_3	5.072	6.430	10.869	7.723	9.748	10.983	7.576	7.883	4.904	4.531	3.866
Al_2O_3/TiO_2	15.192	26.120	9.585	11.494	10.440	9.919	13.577	12.719	11.477	17.474	11.472
K_2O/Na_2O	2.623	2.507	7.566	11.883	6.183	8.266	10.314	5.892	11.552	19.104	31.754

Geochemical data suggest that the Barail sandstones have high SiO_2 values ranging between 69 and 85 wt. % (Table 3). The high SiO_2 contents in the studied sandstone samples reflect their quartz-rich nature, and the average SiO_2/Al_2O_3 ratio (CMI: Chemical maturity index) is 7.24. The examined sandstone samples contain a low average CaO content of 0.516 wt. % and relatively high K_2O content (avg. 2.32 wt. %). Depletion of Na_2O (0.390 wt. %) and relative enrichment of K_2O content in Barail sandstones increase the K_2O /Na_2O ratios, which range from 2.51 to 31.75. Al_2O_3/TiO_2 ratios of the studied samples range from 9.59 to 26.12.

Except for two samples that fall within the shale and Fe-sand categories, Barail sandstones are classed as litharenite and greywacke using Herron's (1988) geochemical diagram (Fig. 8). Binary variation diagrams of SiO_2 versus Al_2O_3, TiO_2, Fe_2O_3, MgO, CaO, and K_2O of all the analyzed samples display similar negative linear trends (Fig. 9). While binary variation diagrams of Al_2O_3 versus TiO_2, Na_2O, K_2O, Fe_2O_3, MgO, and CaO of all the studied samples exhibit the positive linear trends (Fig. 10).

Suttner and Dutta's (1986) bivariant plot of SiO_2 versus Al_2O_3+ K_2O + Na_2O was used to analyze the maturity of the Barail sandstones as a function of climate. Figure 11 shows that most of the lower part sandstone facies (FA1) are derived from semi-humid conditions (relatively high chemical maturity), while the upper part sandstone facies (FA2) are derived from semi-arid conditions (relatively low chemical maturity). Roser and Korsch's (1988) discrimination diagram demonstrates that the analyzed samples are derived from quartzose sedimentary provenance (Fig. 12). Chemical Index of Alteration (CIA), Chemical index of weathering (CIW) and Plagioclase Index of Alteration (PIA) values of the samples range from 56.78 to 85.69 (avg. 79.03), 67.63 to 98.84 (avg. 93.61) and 59.98 to 98.58 (avg. 92.07) (Table 3).

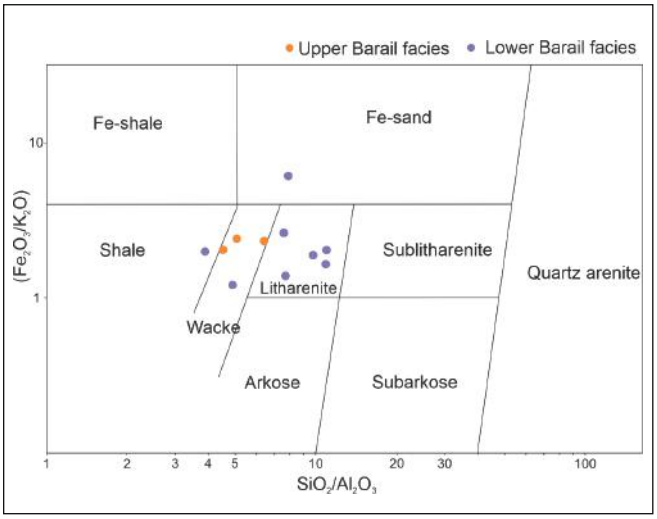

Figure 8: Geochemical Classification of Barail Sandstone Samples Based on the Log (SiO_2/ Al_2O_3)-log (Fe_2O_3/K_2O) Diagram of Herron (1988). Orange-coloured Circles are FA2 Samples, and Blue-colored Circles are FA1 Samples

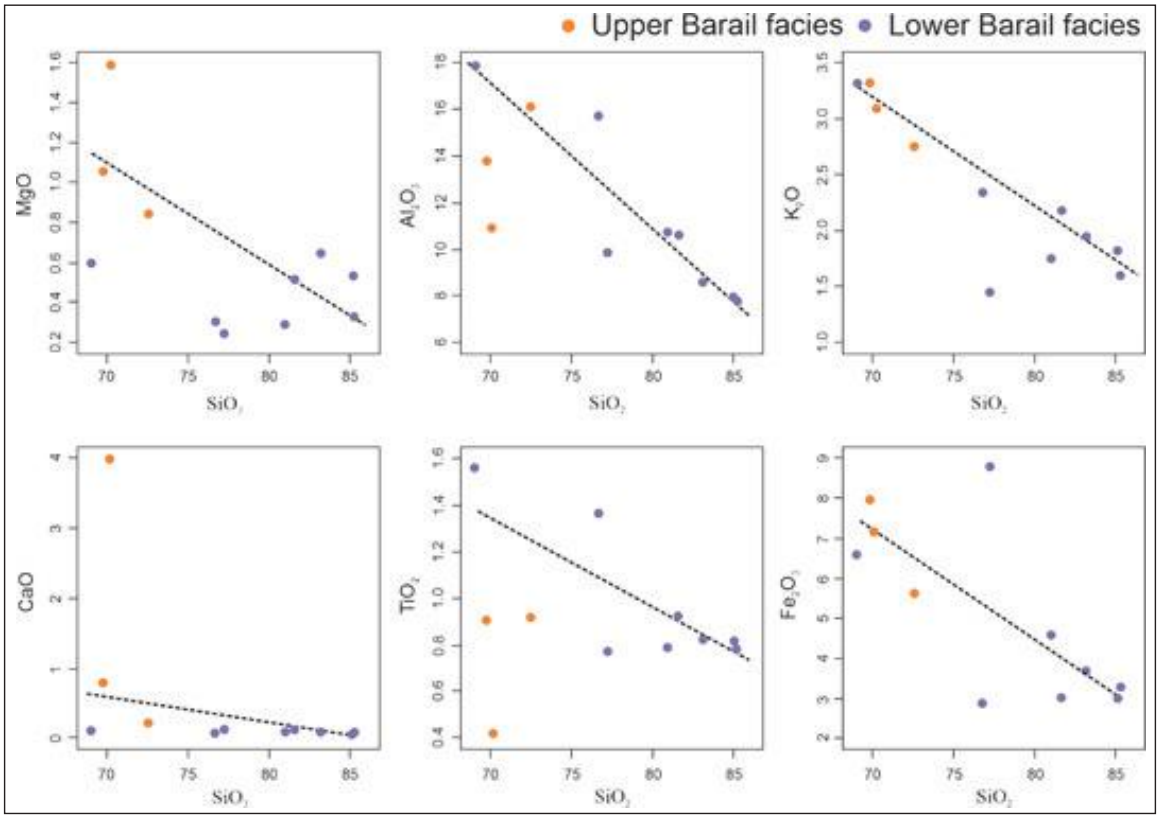

Figure 9: Binary Variation Diagram of Major Oxides vs. SiO_2 Plots of the Barail Sandstones

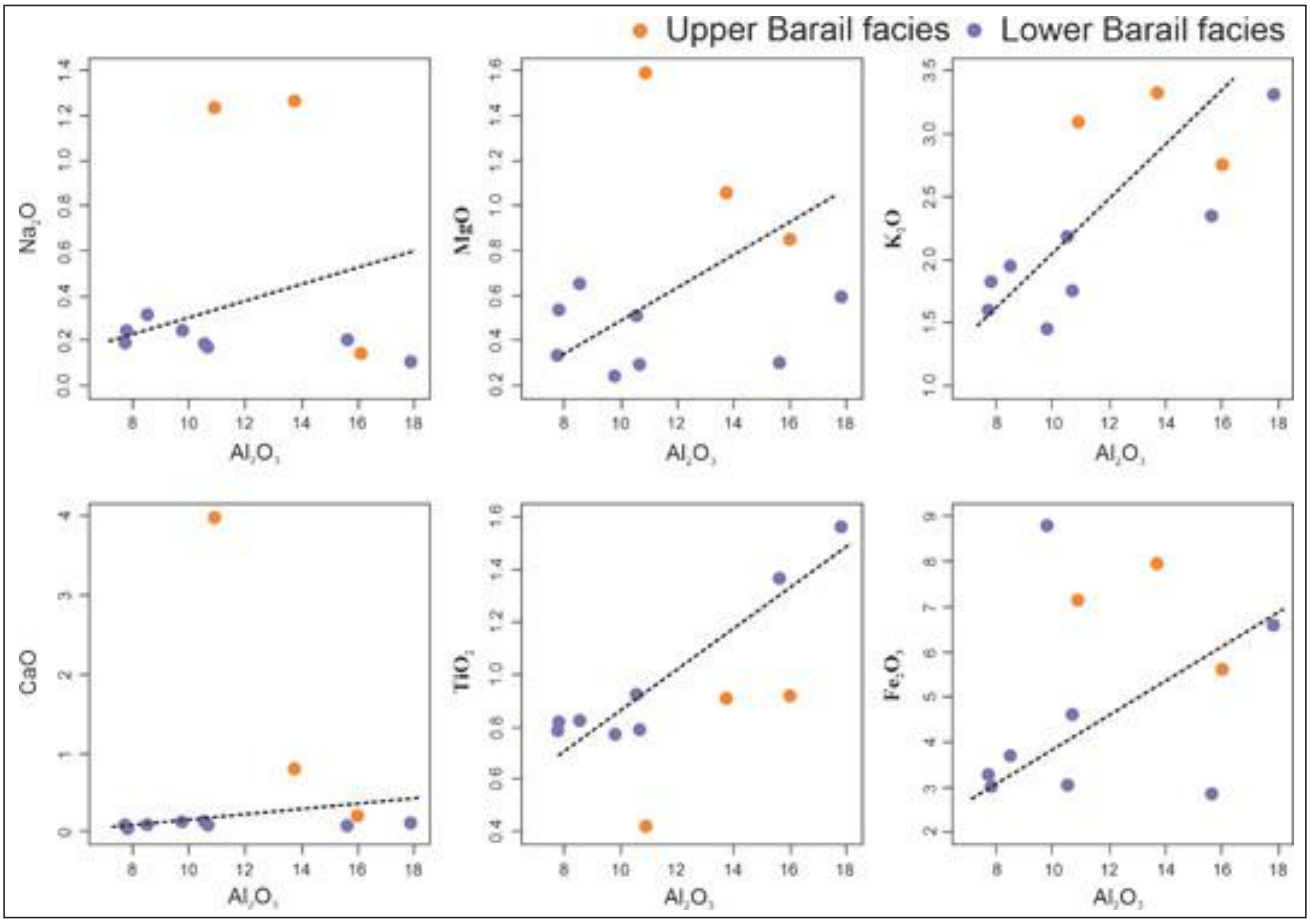

Figure 10: Binary Variation Diagram of Major Oxides vs. Al_2O_3 of the Barail Sandstone

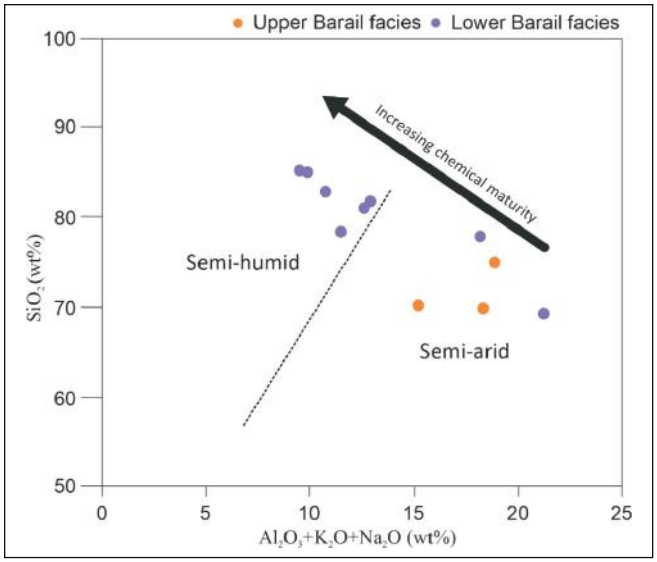

Figure 11: Bivariant Plot of SiO_2 Versus Al_2O_3+K_2O+Na_2O (after Suttner and Dutta, 1986) for Barail Sandstones

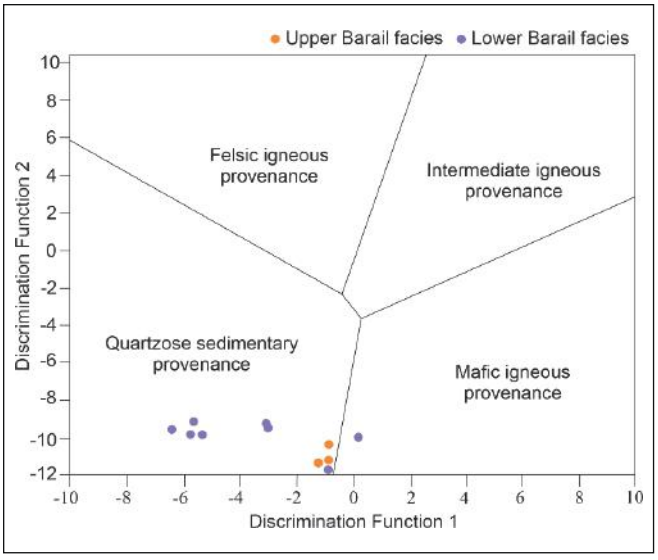

Figure 12: Discrimination Diagram of (Discrimination Function 1 versus Discrimination Function 2) for the Barail Sandstones (after Roser and Korsch, 1988)

DISCUSSION

The sedimentological, petrographic, and geochemical data collected and analyzed during this study allow us to address four issues of the Barail sandstone unit: i) Tectono-provenance, palaeoclimate, and weathering, ii) depositional environment and sandbody stacking pattern, iii) textural properties and diagenesis of sandstones, and iv) implication of the above parameters on reservoir quality. These issues are described in the following sections:

Tectono-provenance, Palaeoclimate, and Weathering

On a regional scale, tectonic settings and palaeoclimate play an essential role in determining the composition and distribution of sandstones (Dickinson and Suczec, 1979). The tectonic discrimination plot (Fig. 6B) indicates that the provenance of the Barail sandstone is recycled orogeny, and the discrimination diagram (Fig. 12) shows they are derived from quartzose sedimentary provenance. These results suggest that sediments of the Barail sandstone were derived from the orogenic belt of the proto-Himalaya in the northern part of the basin. Previous works by Johnson and Alam (1991), Islam et al. (2021), and Borgohain et al. (2010) studied the Barail sandstone in the Surma Basin and suggested that the sediments are derived from the proto-Himalayan orogen and early orogenic belt formed from the collision of the Indian plate and the Burmese plate of the active continental margin provenance.

The QFL (Q: quartz, F: feldspar, and L: lithic grains) plot (Fig. 6A) and Herron's (1988) geochemical plot (Fig. 8) demonstrate that all the sandstone samples contain a high proportion of quartz with less amount of feldspar and a moderate amount of lithic grains which suggests that the sandstones are Litharenite type. The low feldspar contents suggest a long transportation of sediments where most plagioclase feldspars have been transformed into clay minerals during transport (Boggs, 1987). The bivariant plot of SiO_2 versus $Al2O_3$+K_2O+Na_2O (after Suttner and Dutta, 1986) for Barail sandstones shows that the lower part of the succession was deposited in semi-humid while the upper part of the succession shows semi-arid climatic condition. The lower part of the Barail sandstone was deposited in the early Oligocene when the Surma Basin was positioned between 0º–10º latitude when the climatic condition was semi-humid. With time, the basin, along with the Indian plate, moves toward the north and is positioned between 15º–20º latitude. At that time, the height of the Himalayas was not so high, which indicates a semi-arid climatic condition prevailed in the basin.

The chemical index of alteration (CIA), chemical index of weathering (CIW), and plagioclase index of alteration (PIA) values range from 56.78–85.69 (avg. 79.03), 67.63–98.84 (avg. 93.61), and 59.98–98.58 (avg. 92.07), respectively, suggest a moderate to a high degree of source area weathering (Godo et al., 2017; Lucas et al., 2021; McLennan et al., 1993).

Depositional Environment and Sandbody Stacking Pattern

Lithofacies analysis of the studied sections demonstrates that the Barail sandstones were deposited in the tidal-influenced channel to fluvial depositional environments. The poorly laminated mudstone with sand or coal lenses composition of overbank facies association and the smaller sizes of the individual channel deposits with abundant mud drapes in the lower part of the succession suggests that deposition occurred in the delta plain distributary channels and swampy overbank environments. In the upper part of the succession, the presence of massive and cross-stratified sandstones with intraformational conglomerates above the channel scouring surfaces, the coarser grain size, larger bedform, and absence of tidal influence suggest that the fluvial power increases compared to the lower part, which indicates progradation of channel deposits. Johnson and Alam (1991) also suggested that progradational successions were deposited in the Barail sandstone unit during the Oligocene.

Architecturally, the channel bodies in the lower part are comparatively smaller (up to 10m thick and 100m wide) and show mainly multi-storied stacking patterns (Fig. 4A, B, & C). In the upper part, coarser sand grains, intraformational conglomerate, thick (c. 1 meter thick) cross-bedding sets, and >50m thick stacked channel body suggest that channel body dimension is much larger compared to those of the lower part of the succession— indicates a thickening upward sequence (Fig. 4D & 4E). Width/thickness (W/T) ratio plots of Gibling (2006) suggest a 50m thick channel body is at least greater than 1500m wide and forms an

amalgamated multi-storey channel sheet deposit with W/T ratio >15 (Rahman et al., 2022).

Textural Properties and Diagenesis of Sandstones

Sedimentological and petrographic analysis suggest that the Barail sandstone comprises fine to medium-grained, sub-rounded, moderately sorted sandstone. The sub-rounded grains and moderate sorting of the sandstones suggest that the Barail sandstones are texturally moderately mature. Compositionally, the sandstones are of the Litharenite type and have a high proportion of quartz with a minor amount of feldspar and a moderate amount of lithic grains. The litharenite type of the sandstones suggests that they are compositionally submature. The sorting of litarenite sandstones varies from poorly to well-sorted, however, the studied samples show moderately sorted grains.

The diagenetic processes that affected the Barail sandstones are mechanical compaction, cementation, grain bending, fracturing, and dissolution. The presence of line, suture, and concavo-convex contacts indicates a moderate to high level of mechanical compaction during the burial of the sandstone deposits. The presence of slight mica bending and fractured quartz grains suggest the rearrangement of grain fabrics due to burial compaction (Fig. 5). The studied cementing materials are hematite, which may be dissolved and precipitated from the lithic fragments or mafic minerals. The presence of corroded grains represents the dissolution and secondary porosity development. Dissolution of plagioclase feldspars may occur when it comes in contact with acidic fluids, producing a good amount of secondary porosity. The higher standard deviation of porosity percentage in lower Barail sandstone succession (FA1) represents the variable dissolution. On the other hand, the lower standard deviation of the porosity in upper Barail succession (FA2) suggests uniform dissolution.

Implication on Reservoir Quality

This study suggests that both the depositional settings and the diagenetic processes control the reservoir quality of the Barail sandstone. The sedimentary facies significantly influence the composition and texture of sandstone, which is directly related to reservoir quality. The fine to medium grain size, sub-rounded grain shape, moderate sorting, and porosity values (avg. 16.9%) suggest that the Barail sandstones are an excellent reservoir. However, the reservoir properties are not equally distributed throughout the succession. The higher standard deviation of porosity values (porosity values range from 8–22%) of the tidal-influence channel deposits (FA1) compared to the moderate standard deviation (porosity values range from 16–22%) of the fluvial channel deposits (FA2) suggests that FA2 is less heterogeneous than FA1. Depositional settings also play an essential role in determining the size of the reservoir—another important reservoir property. The sandbody dimension in the upper part (FA2) of the succession is larger than the lower part (FA1).

The grain contacts are mainly point and long, with a significant amount of sutured and concavo-convex contacts, indicating moderate to high compaction. The bending of mica flakes is also evidence of mechanical compaction and the packing re-adjustment. The ferrugineous and calcareous cementing materials and quartz overgrowth decreased the pore space and occluded pore-to-pore contact. In the burial depth, due to mechanical compaction and cementation, the primary porosity and permeability of the sandstones decreased with depth. However, the dissolution process produced a significant amount of secondary porosity, which increased the total porosity percentage of the succession. The geochemical analysis suggests that the sandstones are chemically stable and moderately mature, which is necessary for the reservoir rock. The study indicates that the Barail sand units may act as a good-quality reservoir rock.

CONCLUSIONS

In the present study, detailed sedimentological, petrographic, and geochemical analyses of the Barail sandstones are performed to investigate their reservoir quality. Three facies associations: Tidal-influenced multistorey channel facies association (FA1), Fluvial multistorey channel facies association (FA2), and Overbank facies association (FA3) are observed in the study area, which indicates the Barail sandstone formation was likely deposited delta plain to the fluvial environment. The channel sand units of distributaries (FA1 and FA2) are prospective reservoir rocks. The individual channel dimensions and channel body width and thickness increase toward the top of the formation. Petrographic analysis suggests that the channel

deposits are quartz-rich, feldspar-poor, and have lithic fragment populations dominated by sedimentary and metamorphic clasts with poor mud clasts and were derived from a recycled orogeny. The petrographic analysis also suggests that these sandstones have sufficient pore spaces (avg. porosity 16.9 %) and the pores are interconnected. Porosity distribution in the upper part of the succession is less heterogeneous than the lower part and has higher reservoir potential. Geochemically, the Barail sandstone unit is moderately mature and stable because of the high silica percentage. The sandstones have gone under a moderate degree of alteration. Although the mechanical compaction and cementation process decreases the porosity, the dissolution process creates secondary porosity in the sandstone. The study suggests that the Barail sandstone unit has an excellent potential to act as a reservoir, which may provide new hope for petroleum exploration in Bangladesh.

ACKNOWLEDGEMENT

The research was funded by the Bangladesh Bank and the Faculty of Earth and Environmental Sciences. We are indebted to the Department of Geology, University of Dhaka, and IMMM (BCSIR) for providing laboratory support.

REFERENCES

Alam, M., 1989. Geology and depositional history of Cenozoic sediments of the Bengal Basin of Bangladesh. Palaeogeography, Palaeoclimatology, Palaeoecology 69(C), 125–139. https://doi.org/10.1016/0031-0182(89)90159-4.

Alam, M., Alam, M. M., Curray, J. R., Chowdhury, M. L. R., Gani, M. R., 2003. An overview of the sedimentary geology of the Bengal Basin in relation to the regional tectonic framework and basin-fill history. Sedimentary Geology 155(3–4), 179–208. https://doi.org/10.1016/S0037-0738(02)00180-X.

Boggs, S. Jr., 1987. Principles of sedimentology and stratigraphy. New York: Macmillan Publishing Company, 784.

Borgohain, K., Borgohain, P., Bharali, B., Baruah, J., 2019. Sedimentological characteristics of the barail arenaceous unit of makum-north Hapjan oil field, Assam. International Journal of Earth Science and Geology 1(2), 66–73.

Borgohain, P., Borah, C., Gilfellon, G. B., 2010. Sandstone diagenesis and its impact on reservoir quality of the arenaceous unit of Barail Group of an oilfield of upper Assam shelf, India. Current Science 82–88.

Borgohain, P., Bezbaruah, D., Gogoi, M. P., Gogoi, Y. K., Phukan, P. P., Bhuyan, D., 2021. Petrography and diagenetic evolution of the Barail sandstones of Naga Schuppen belt, North East India: implication towards reservoir quality. Current Science 121(8), 1107.

Curray, J. R., Emmel, F. J., Moore, D. G., 2002. The Bengal Fan: morphology, geometry, stratigraphy, history and processes. Marine and Petroleum Geology 19(10), 1191–1223.

Dickinson, W. R., Suczek, C. A., 1979. Plate tectonics and sandstone compositions. American Association of Petroleum Geologists' Bulletin 63, 2164–2182.

Dickinson, W. R., 1985. Interpreting provenance relations from detrital modes of sandstones. Provenance of arenites 333–361.

Dott, R. H., 1964. Wacke, graywacke and matrix; what approach to immature sandstone classification? Journal of Sedimentary Research 34(3), 625–632.

Evans, P., 1932. Tertiary succession in Assam. Trans. Min. Geol. Inst. India 27, 155 – 260.

Evans, P., 1964. The tectonic framework of Assam. Geological Society of India 5, 80-96.

He, J., Wang, H., Zhang, C., Yang, X., Shangguan, Y., Zhao, R., Gong, Y., Wu, Z., 2019. A comprehensive analysis of the sedimentology, petrography, diagenesis and reservoir quality of sandstones from the Oligocene Xiaganchaigou (E 3) Formation in the Lengdong area, Qaidam Basin, China. Journal of Petroleum Exploration and Production Technology 9(2), 953–969. https://doi.org/10.1007/s13202-018-0571-z

Ghosh, S., Guchhait, S. K., 2015. Characterization and evolution of laterites in West Bengal: Implication on the geology of northwest Bengal Basin. Transactions 37(1), 93-119.

Gibling, M. R., 2006. Width and thickness of fluvial channel bodies and valley fills in the geological

record: A Literature Compilation and Classification. Journal of Sedimentary Research 76, 731–770, https://doi.org/10.2110/jsr.2006.060.

Godoy, L. H., Sardinha, D. D. S., Moreno, M. M. T., 2017. Major and trace elements redistribution in weathered claystones from the Corumbataí Formation, Paraná Sedimentary Basin, São Paulo, Brazil. Brazilian Journal of Geology 47, 615-632.

Hiller, K., Elchi, M., 1984, February. Structural development and hydrocarbon entrapment in the Surma basin/Bangladesh (northwest Indo Burman fold belt). In Southeast Asia Show. OnePetro.

Herron, M. M., 1988. Geochemical classification of terrigenous sands and shales from core or log data. Journal of Sedimentary Research 58(5), 820-829.

Hossain, H. M. Z., Roser, B. P., Kimura, J. I., 2010. Petrography and whole-rock geochemistry of the Tertiary Sylhet succession, northeastern Bengal Basin, Bangladesh: Provenance and source area weathering. Sedimentary Geology 228(3-4), 171-183.

Imam, B., 2013. Energy resources of Bangladesh. Second Edition, University Grants Commission of Bangladesh, Dhaka, Bangladesh.

Islam, M. S., Shijan, M. H. H., Saif, M. S., Biswas, P. K., Faruk, M. O., 2021. Petrophysical and petrographic characteristics of Barail Sandstone of the Surma Basin, Bangladesh. Journal of Petroleum Exploration and Production, May. https://doi.org/10.1007/s13202-021-01196-0.

Johnson, S. Y., Alam, A. M. N., 1991. Sedimentation and tectonics of the Sylhet trough, Bangladesh. Geological Society of America Bulletin, 103(11), 1513–1527. https://doi.org/10.1130/0016-7606(1991)103<1513:SATOTS>2.3.CO;2.

Khanam, F., Rahman, M. J. J., Alam, M. M., Abdullah, R., 2021. Sedimentology and basin-fill history of the Cenozoic succession of the Sylhet Trough, Bengal Basin, Bangladesh. International Journal of Earth Sciences 110(1), 193–212. https://doi.org/10.1007/s00531-020-01946-1.

Lietz. J. K., Kabir, J., 1982. Prospects and constraints of oil exploration in Bangladesh: Singapore, Fourth Offshore Southeast Asia Conference, p. 1-6.

Lucas, F. A., Fregene, T. J., 2021. Geochemical maturity and paleo-weathering indices of sedimentary succession in JV field greater ughelli depo-Belt Niger Delta Basin. Journal of Applied Sciences and Environmental Management 25(5), 773-777.

Martin, C. A., Turner, B. R., 1998. Origins of massive-type sandstones in braided river systems. Earth-Science Reviews 44(1-2), 15-38.

McBride, E. F., 1963. A classification of common sandstones. Journal of Sedimentary Research 33(3), 664-669.

McLennan, S. M., Hemming, S., McDaniel, D. K., Hanson, G. N., 1993. Geochemical approaches to sedimentation, provenance, and tectonics. Special Papers-Geological Society of America 21-21.

Noori, A., Rais, S., 2014. Geochemistry and detrital modes of sandstone from barakar formation in Mand Valley Basin, Chhattisgarh, India: Implications for provenance, tectonic setting and paleoweathering. International Journal of Basic and Applied Sciences 3(2), 124.

Parvin, A., Woobaidullah, A. S. M., Rahman, M. J., 2019. Sequence stratigraphic analysis of the Surma Group in X Gas Field, Surma Basin, Bengal Delta. Journal of Nepal Geological Society 58, 39–52. https://doi.org/10.3126/jngs.v58i0.24572.

Rahman, M. M., Howell, J. A., Macdonald, D. I. M., 2022. Virtual outcrop-based analysis of channel and crevasse splay sandstone body architecture in the middle jurassic ravenscar group, Yorkshire, NE England, https://doi.org/10.1144/jgs2021-017.

Reimann, K. U., Hiller, K., 1993. Geology of Bangladesh.

Roser, B. P., Korsch, R. J., 1988. Provenance signatures of sandstone-mudstone suites determined using discriminant function analysis of major-element data. Chemical Geology 67(1-2), 119-139.

Suttner, L. J., Dutta, P. K., 1986. Alluvial sandstone composition and paleoclimate; I, Framework mineralogy. Journal of Sedimentary Research 56(3), 329-345.

Srivastava, S. K., Pandey, N., 2011. Search for provenance of Oligocene Barail sandstones in and around Jotsoma, Kohima, Nagaland. Journal of the Geological Society of India 77(5), 433–442. https://doi.org/10.1007/s12594-011-0045-0.

Srivastava, S. K., Kichu, A. M., 2022. Mineral assemblages and tectono-provenance of the Oligocene Barail sandstones in parts of Naga Hills of the Assam-Arakan Orogenic Belt, North-east India. Geological Journal 57(2), 801-817.

Shofiqul, I. M., Nusrat, J. L., 2013. Reservoir characterization of Habiganj gas field. International Journal of Oil, Gas and Coal Engineering 1(1), 7-15.

Tamrakar, N. K., Syangbo, D. K., 2014. Petrography and provenance of the Siwalik Group sandstones from the main boundary thrust region, Samari River area, central Nepal, sub-Himalaya. Boletin de Geologia 36(2), 25–44.

Trendell, A. M., Atchley, S. C., and Nordt, L. C., 2012. Depositional diagenetic controls on reservoir attributes within a fluvial outcrop analog: Upper Triassic Sonsela member of the Chinle Formation, Petrified Forest National Park, Arizona. AAPG Bulletin 96(4), 679-707.

Uddin, A., Lundberg, N., 1998. Cenozoic history of the Himalayan-Bengal system: Sand composition in the Bengal basin, Bangladesh. Geological Society of America Bulletin 110(4), 497-511.